AMERICAN SOCIETY FOR MICROBIOLOGY | Antimicrobial Agents and Chemotherapy®

ANTIVIRAL AGENTS

An Enhanced Emtricitabine-Loaded Long-Acting Nanoformulation for Prevention or Treatment of HIV Infection

Subhra Mandal,[a] Michael Belshan,[b] Ashley Holec,[a,b] You Zhou,[c] Christopher J. Destache[a]

Department of Pharmacy Practice, School of Pharmacy and Health Professions, Creighton University, Omaha, Nebraska, USA[a]; Department of Medical Microbiology & Immunology, Creighton University School of Medicine, Creighton University, Omaha, Nebraska, USA[b]; Center for Biotechnology, University of Nebraska-Lincoln, Lincoln, Nebraska, USA[c]

ABSTRACT Among various FDA-approved combination antiretroviral drugs (cARVs), emtricitabine (FTC) has been a very effective nucleoside reverse transcriptase inhibitor. Thus far, FTC is the only deoxycytidine nucleoside analog. However, a major drawback of FTC is its large volume distribution (averaging 1.4 liters/kg) and short plasma half-life (8 to 10 h), necessitating a high daily dosage. Thus, we propose an innovative fabrication method of loading FTC in poly(lactic-co-glycolic acid) polymeric nanoparticles (FTC-NPs), potentially overcoming these drawbacks. Our nanoformulation demonstrated enhanced FTC loading (size of <200 nm and surface charge of −23 mV) and no to low cytotoxicity with improved biocompatibility compared to those with FTC solution. An *ex vivo* endosomal release assay illustrated that NP entrapment prolongs FTC release over a month. Intracellular retention studies demonstrate sustained FTC retention over time, with approximately 8% (24 h) to 68% (96 h) release with a mean retention of ~0.74 μg of FTC/10^5 cells after 4 days. An *in vitro* HIV-1 inhibition study demonstrated that FTC-NP treatment results in a 50% inhibitory concentration (IC_{50}) ~43 times lower in TZM-bl cells (0.00043 μg/ml) and ~3.7 times lower (0.009 μg/ml) in peripheral blood mononuclear cells (PBMCs) than with FTC solution (TZM-bl cells, 0.01861, and PBMCs, 0.033 μg/ml). Further, on primary PBMCs, FTC-NPs also illustrate an HIV-1 infection blocking efficacy comparable to that of FTC solution. All the above-described studies substantiate that FTC nanoformulation prolongs intracellular FTC concentration and inhibition of HIV infection. Therefore, FTC-NPs potentially could be a long-acting, stable formulation to ensure once-biweekly dosing to prevent or treat HIV infection.

KEYWORDS antiretroviral drug, emtricitabine, nanoparticles, HIV infection, ARV drug, PLGA polymer

Received 7 July 2016 **Returned for modification** 12 August 2016 **Accepted** 31 October 2016

Accepted manuscript posted online 7 November 2016

Citation Mandal S, Belshan M, Holec A, Zhou Y, Destache CJ. 2017. An enhanced emtricitabine-loaded long-acting nanoformulation for prevention or treatment of HIV infection. Antimicrob Agents Chemother 61:e01475-16. https://doi.org/10.1128/AAC.01475-16.

Address correspondence to Subhra Mandal, SubhraMandal@creighton.edu, or Christopher J. Destache, ChrisDestache@creighton.edu.

Worldwide, antiretroviral therapy has markedly improved the morbidity and mortality associated with human immunodeficiency virus (HIV)-infection. Evidence that patients receiving antiretroviral therapy have significant reduction in hospitalizations and improved survival is accumulating (1). Antiretroviral therapy has made HIV a manageable, chronic infection, with the caveat that patients must maintain high medication adherence (2). According to WHO and UNAIDS (as of 2014), globally about 36.9 million people are living with HIV infection (3).

In current combination antiretroviral (cARV) drug regimens, tenofovir (TFV) and emtricitabine (FTC) are two FDA-approved nucleoside reverse transcriptase inhibitors (NRTIs) that, along with drugs from other classes, are designated the preferred therapy for initial treatment of HIV-1 (4). The effectiveness of these two NRTIs can be attributed to their high tolerability and patient acceptability (3). High patient tolerability for TFV

and FTC drugs has led to their inclusion in the Department of Health and Human Services preferred once-daily cARV drug regimen in combination with other classes (4–6). However, to enhance adherence, the once-daily dosing requires a large (milligram) dose that increases the risk of severe side effects. Additionally, the high dose has wide fluctuations between peak and trough levels within the dosing interval. These factors contribute to reduced adherence of ARV drugs for HIV-1 treatment. Nonadherence can be linked to the development of HIV-1 resistance (6).

To improve adherence to therapy, investigators are utilizing pharmaceutical nanotechnology. In ARV encapsulations into a nanoparticle formulation, drugs are released from the nanoparticles over an extended period, allowing for once-monthly or longer treatment modalities (7–9). However, the encapsulation of water-soluble ARV drugs, namely, NRTIs such as FTC, has been difficult, and the encapsulation efficiency has been quite low (10). Our laboratory has been working on solving this problem. This article reports a unique technique for FTC nanoformulation into poly(lactic-co-glycolic acid) polymer, a biodegradable/biocompatible polymeric nanoparticle that shows high FTC encapsulation efficiency and has enhanced HIV-1 inhibition efficacy. The current FTC nanoformulation can be useful as long-acting nanoparticles (NPs) for both HIV-1 treatment and prevention.

RESULTS

Characterization of NPs. As FTC is a hydrophilic drug, the water-in-oil-in-water (W-O-W) double emulsion solvent evaporation method was followed to ensure its potential encapsulation in the poly(lactic-co-glycolic acid) (PLGA) NPs (Fig. 1) (11). The physiochemical characteristics of FTC-NPs are summarized in Table 1. The analysis demonstrates that NP obtained are $<$200 nm diameter and possess narrow size distribution (polydispersity index [PDI] $<$ 0.2). The scanning electron microscopy (SEM) image reveals the NPs have uniform and smooth spherical surface (Fig. 1).

Even though FTC-NPs can be prepared by directly dissolving FTC in aqueous solution, we found and it has been reported previously (10) that dissolving water-soluble drugs in buffer pH over their pK_a value enhances drug loading (DL) efficiency. We found that 1 mM HEPES buffer (pH 9) leads to enhanced FTC loading in NPs. Furthermore, use of a stabilizer ensures particle stability and control release characteristics (11, 12). Use of 1 mM HEPES buffer (pH 9) (primary aqueous phase) and 1% polyvinyl alcohol (PVA) solution (secondary aqueous phase) as aqueous phases and PF-127 as an organic phase stabilizer along with PLGA results in enhanced drug loading, longer stability, and uniform size NPs (9, 13). The percent encapsulation efficiency (EE) and percent DL of FTC in FTC-NP were enhanced to 50.6% $\pm$ 5.5% and 4.2% $\pm$ 1.2%, respectively ($n = 7$). The encapsulation efficiency shows that PLGA NP entrapment enhances FTC drug solubility compared to that obtained with FTC aqueous medium nanoparticle entrapment (http://www.drugbank.ca/drugs/DB00879).

FTC-NP *in vitro* cytotoxicity. Free FTC drug solution has been shown to have minimal cellular cytotoxicity (14). However, nanoformulation of FTC adds a new chemical entity requiring proper evaluation of FTC encapsulated nanoparticles for cytotoxicity prior to determining functionality. We chose the HeLa cell line to mimic the endothelial cells as well as female cervical cells (15), the first cell type that NPs encounter after subcutaneous, intravenous, or intravaginal administration. However, in order to evaluate the cytotoxicity of ARV drugs at the target site or reservoirs such as T lymphocytes, we selected the H9 cell line (16), and to evaluate cytotoxicity effect on primary cells, we isolated human peripheral blood mononuclear cells (PBMCs) to compare cell viabilities with FTC-NP and FTC solution. The H9 and HeLa cell viability assay results (Fig. 2) indicate that FTC-NPs are nontoxic, similar to the findings with FTC solution and untreated cells at concentrations as high as 10 μg/ml of FTC (Fig. 2A and B) and after 24 h and 96 h of treatment (Fig. 2D and E).

Further, to evaluate the selectivity index (SI) on primary target cell type, we determined the cytotoxic concentration that caused death of 50% of viable cells (CC_{50}).

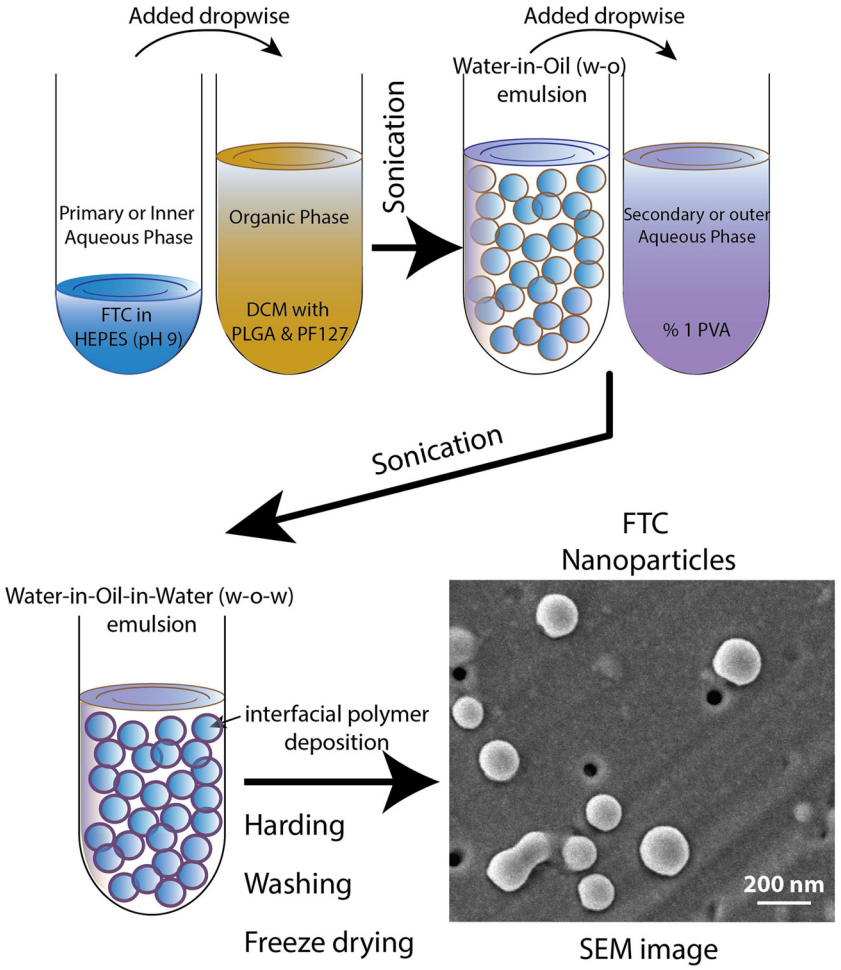

FIG 1 Schematic diagram providing a stepwise explanation of FTC-NP formulation by the W-O-W interfacial polymer deposition method. At the extreme right bottom is a representative SEM image showing FTC-NP overall morphology.

The PBMC viability was tested at 50, 5, 0.5, 0.05, and 0.005 μg/ml, and the SIs were determined by equation 1:

$$\mathrm{SI} = \mathrm{CC}_{50}/\mathrm{IC}_{50} \quad (1)$$

where IC_{50} is the 50% inhibitory concentration.

The results (Fig. 2C) comparing FTC-NP and FTC solution demonstrated nonsignificant ($P > 0.05$) cytotoxicity at the highest concentrations (50 μg/ml at 96 h of incubation). Thus, FTC nanoencapsulation does not demonstrate an elevated cytotoxic effect in endothelial cells, lymphocytes, or human PBMCs.

Intracellular retention. The main objectives for the use of a nano-drug carrier system are to enhance drug uptake, increase drug retention, and generate slow but controlled release over time. To evaluate the attainment of these objectives, intracel-

TABLE 1 FTC-NP physiochemical characteristics[a]

FTC-NP characteristic	Value
Particle size (nm)	175.9 ± 24.7
Zeta potential (mV)	−25.6 ± 1.94
PDI	0.145 ± 0.028
% EE	53.8 ± 5.07
% DL	4.9 ± 1.6

[a]All data are presented as means ± SE for 6 independent FTC-NP batches.

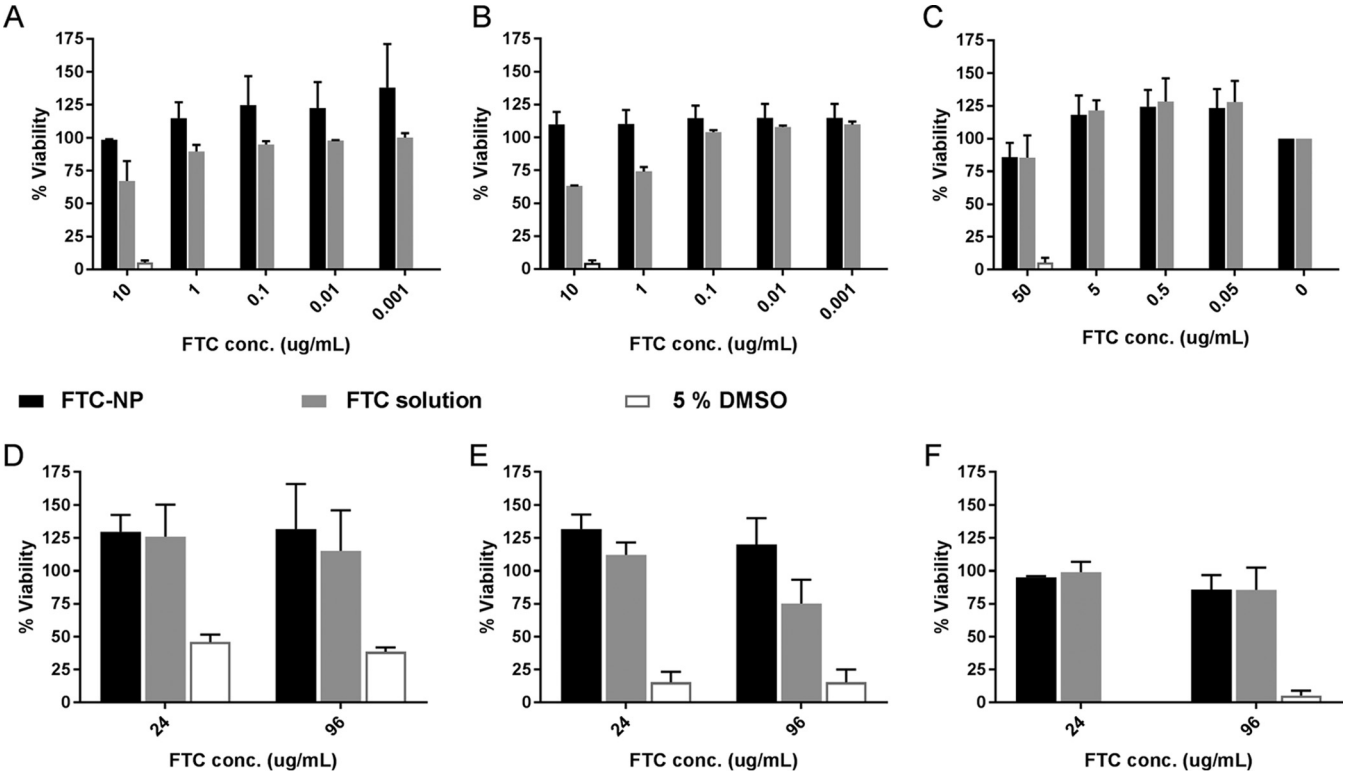

FIG 2 Cytotoxicity assay on HeLa cells (A and D), H9 cells (B and E), and PBMCs (C and F) at different treatment concentrations (A to C) after 96 h of treatment and at the highest concentration (10 μg/ml for HeLa and H9 cells and 50 μg/ml for PBMCs) over different periods (D to F). Data are represented as means ± SE for 3 independent experiments performed in triplicate.

lular retention efficiency was estimated at different intervals using TZM-bl cells (Fig. 3). The 24-h FTC-NP treatment shows no significant difference in overall uptake and retention compared to FTC solution. However, FTC-NP-treated cells displayed significant FTC retention (>60%) after 48-h and 96-h treatment intervals ($P < 0.001$). This observation confirms that nanoencapsulation of FTC increases the intracellular concentrations within the cells.

Endosomal pH release study. To assess the NP entrapped FTC release efficacy at endosomal subunit of cell, we studied the FTC release kinetics from FTC-NP (47.5 μg of FTC entrapped in 5-mg NPs) at pH 5.5 (Fig. 4). The study revealed that ~62% of FTC is released within 1 h of incubation. However, after 1 h of release, there is a relatively constant FTC release over 14 days. By 30 days, the NP releases ~85% of its FTC content. After 30 days, the remaining FTC-NPs still have ~10% FTC entrapped in FTC-NPs. The

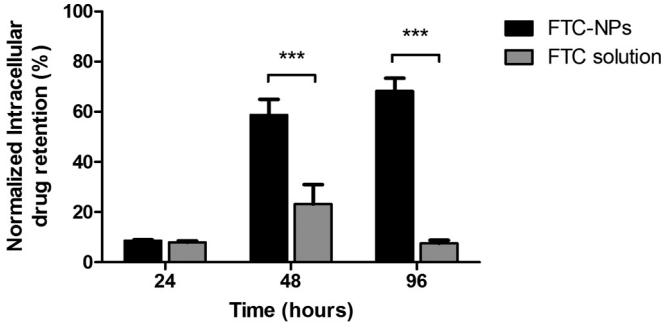

FIG 3 FTC release efficiency analysis over different periods (24 h, 48 h, and 96 h). The data were normalized against those for the untreated sample and represent means ± SE from 3 independent experiments. ***, $P < 0.001$.

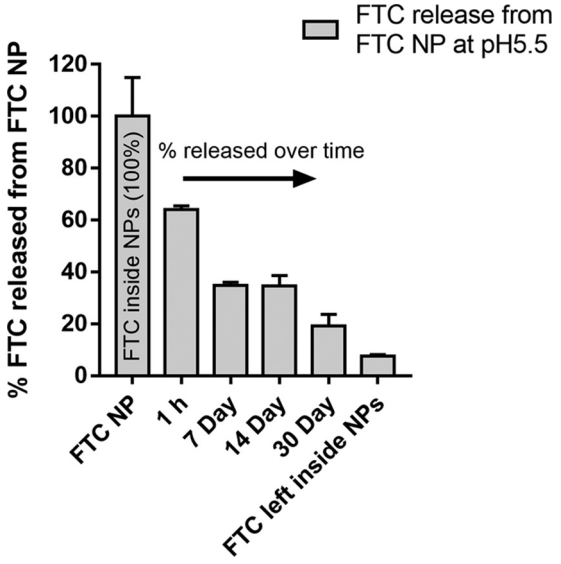

FIG 4 Endosomal low pH (pH 5.5) release study of FTC from FTC-NPs. The data represent percent FTC release, considering the FTC concentration in 5 mg/ml of FTC-NPs as 100%. Each data point represents the mean ± SE for FTC release from three independent FTC-NPs batches.

one-phase decay analysis estimates that the FTC release half-life is 146.2 h (approximately 6 days). These results document the sustained release properties of the W-O-W emulsion nanoformulation.

***In vitro* prophylaxis studies.** To evaluate the antiretroviral properties of FTC entrapped in NPs, we performed a short-term prophylactic study on TZM-bl indicator cells and PBMCs (Fig. 5). The results of the *in vitro* HIV-1 prophylaxis study indicate that the IC_{50} of the FTC-NPs was as low as 0.00043 μg/ml and that of FTC solution was 0.01861 μg/ml (Fig. 5A). Therefore, FTC-NPs demonstrate an efficacy ~43 times higher than that of FTC solution. However, in PBMCs infected with HIV-1_{LUC} after 96 h of infection (Fig. 5B), again the IC_{50} of FTC-NP was ~3.7-fold lower (0.009 μg/ml) than that of the FTC solution (0.033 μg/ml). Finally, the SI (equation 1) was calculated to be 5,555. These results suggest that a high FTC intracellular concentration (Fig. 3) adds to the efficacy of FTC-NPs preventing HIV-1 infection in TZM-bl cells and PBMCs compared to FTC solution at a low (nanogram) concentration. These results demonstrate that nanoformulation improves the intracellular delivery, retention, and controlled release of FTC for sustained protection from HIV-1 challenge.

To further assess the efficacy of the FTC-NPs, we performed exogenous reverse transcriptase (exo-RT) inhibition studies using primary PBMCs. As Fig. 6 demonstrates,

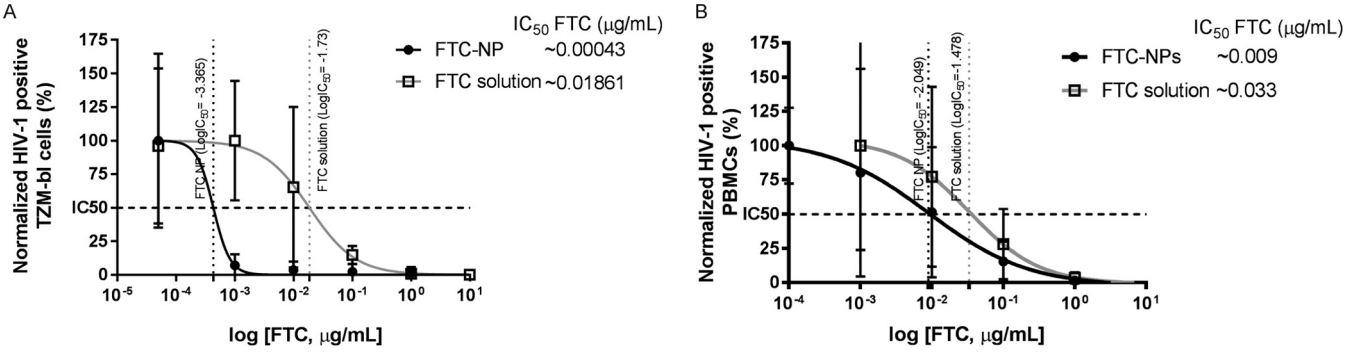

FIG 5 Study of *in vitro* HIV-1 prophylaxis induced by FTC-NPs at different concentrations. (A) TZM-bl cell treatment was done at concentrations of 0.00005, 0.001, 0.01, 1, and 10 μg/ml; (B) PBMC treatment was done at concentrations of 0.005, 0.05, 0.5, 5, and 50 μg/ml. The data were normalized against those for the untreated but infected sample. The *x* values were first transformed to their respective log values, and then IC_{50} was calculated by using the log(agonist)-versus-response equation. The results are represented as means ± SE from 3 independent experiments.

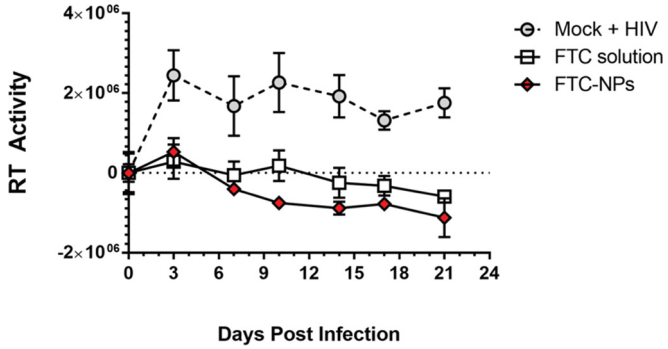

FIG 6 FTC-NP inhibition of HIV-1 RT activity at 500 ng/ml of FTC-NPs compared to 500 ng/ml of FTC solution and PBS (mock) treatment in PBMCs. The data were normalized against those for an untreated uninfected PBMC sample. The *y* values represent RT activity based on amount of [^{32}P]TTP incorporated at respective time points. The results are represented as means ± SE from 2 independent experiments performed in triplicate.

the FTC-NPs prevented virus infection similar to FTC solution even after challenge with HIV-1 and propagation for 21 days. This result validated that FTC-NPs inhibit HIV infection *in vitro* with an efficacy comparable to that of FTC solution. The results indicate that FTC entrapment into the nanoformulation does not interfere with FTC's NRTI functionality.

DISCUSSION

FTC is widely used as a core component of the dual NRTI backbone in all preferred first-line antiretroviral combinations therapies. The major advantage of FTC (a synthetic analog of cytosine) is that its active metabolite FTC-5′triphosphate is a weak inhibitor of mammalian mitochondrial DNA polymerase-γ (17–19). Therefore, FTC is evidently nontoxic to mitochondria. Also it completely lacks uritine-5′-diphosphoglucuronyl transferase as well as cytochrome P450 enzyme inhibition ability (20). The antiretroviral efficacy of FTC for treating both naive and experienced patients has been demonstrated in clinical trials (21, 22). Thus, FTC is one of the most common drugs in the various cARV drug combinations that have shown synergistic inhibition of HIV-1. FTC has shown an additive synergistic effect with other integrase strand transfer inhibitors (INSTI), e.g., elvitegravir or dolutegravir, nonnucleoside reverse transcriptase inhibitors (NNRTI), e.g., efavirenz or rilpivirine, and protease inhibitors, e.g., darunavir (23). FTC has already been made commercially available by Gilead Sciences alone as Emtriva as well as in a double-drug combination tablet (Truvada) (24).

Various studies are ongoing to prolong FTC plasma half-life. There are various combination nanoformulations that have been reported (7, 8, 12, 25–29). Freeling et al. produced solid lipid nanoparticles containing boosted lopinavir (L/r) and TFV. Using macaque model, the investigators demonstrated enhanced penetration of the ARV drugs into lymph nodes compared to that of free drugs (10, 27). Other investigators have used wet-milled technique to develop FTC crystals that boosted protease inhibitor efficacy in humanized mice when linked with folic acid (28, 29). Recently, the LATTE-2 study, administering long-acting cabotegravir and rilpivirine intramuscularly every 2 months or every month, has announced positive results (30).

A recent review and meta-analysis of FTC and lamivudine documented no differences in long-term outcomes for patients receiving either FTC or lamivudine (31). Additionally, FTC and other preferred NRTIs (lamivudine and TFV) have less mitochondrial toxicity than do other NRTIs used in the past. Gastrointestinal symptoms are still side effects associated with NRTIs, but they can be managed. Clinicians are calling for more optimization and simplification of ARV therapies in both adults and children (32). Certainly, treatment simplification will aid in improvement in treatment efficacy and will improve long-term retention in care. Finally, FTC and TFV are FDA approved for preexposure prophylaxis in non-HIV-infected people with multiple risk factors (33). As

prevention, it is a part of a comprehensive set of tools requiring discussion and care for those at high risk. The major drawback of FTC is its high water solubility and high renal clearance plus cross-resistance (33). As a result, a high daily dosage is needed. Therefore, we formulated a method to encapsulate FTC into NPs, i.e., FTC-NPs, that demonstrates improved preexposure prophylaxis in *in vitro* assays, indicating their potential for further study.

The nanoformulation of FTC resulted in enhanced loading of FTC, a water-soluble NRTI drug, and sustained drug release properties. FTC-NPs were formulated by using the W-O-W emulsification method. Physicochemical property analysis (Table 1) revealed that FTC-NPs are small enough (<200 nm) to avoid fine-capillary blockage (34) and exhibit enhanced ARV drug loading efficiency. Further FTC-NPs shows sustained FTC delivery (Fig. 3 and 4). The *in vitro* intracellular retention study demonstrates (Fig. 3) that FTC solution accumulates to ~23% after 48 h, which decreases to ~10% after 96 h. This could be due to the multidrug efflux pump, which induces continuous drug removal from the cell (35). In contrast, the FTC retention profile after 96 h for FTC-NP treatment shows that over 60% FTC gets retained intracellularly.

Further, the study of FTC release from FTC-NP (Fig. 4) reveals that once in the endosome, FTC-NPs show an initial sporadic burst of FTC release (~62% release in 1 h), which can aid in developing the preliminary cellular effective concentration to block RT activity. Further, the endosomal release patterns are more controlled and sustained. After 30 days of incubation, approximately 85% of the FTC was released from FTC-NPs. Therefore, controlled release of FTC from the polymeric NPs in the endosome and retention at the *in vitro* level, enhancing the intracellular level, prolong FTC NRTI functionality.

The study of the efficacy of FTC after release from FTC-NPs in two *in vitro* infection models showed that FTC entrapped in NPs has an inhibitory concentration ~3.7 to 43 times lower than that of free FTC (in solution) (Fig. 5) and is as effective in blocking HIV-1 exo-RT activity as freely soluble FTC (Fig. 6). These studies suggest that NP entrapment induces initial burst release of drug followed by a controlled release over time that maintains high intracellular FTC concentrations and provides effective inhibition of HIV-1 infection. It will be of interest to measure the FTC-triphosphate active metabolite in macrophages, monocytes, and lymphocytes from FTC-NPs compared to FTC solution.

As nonadherence is the main reason that HIV patients fail regimens, any sustained-release treatment modality will potentially improve nonadherence. Further exploration of long-acting nanomedicines would be fruitful for patients that have difficulties with adherence. Extension of the present results to the clinical level for *in vivo* studies, such as pharmacokinetics and efficacy studies in animal models, is needed. However, the present nanoformulation of FTC potentially could be an efficient sustained-release nanodelivery system both for HIV-1 prevention and as part of a treatment strategy. Thus, our next goal is to substantiate present nano-drug delivery system in the preclinical models such as in humanized mice and macaques.

MATERIALS AND METHODS

Materials. PLGA (75:25 lactide/glycolide ratio; M_w, 4,000 to 15,000), polyvinyl alcohol (PVA) (M_w, 13,000 to 23,000), dichloromethane (DCM), acetonitrile (ACN), potassium dihydrogen phosphate (KH_2PO_4), 4-(2-hydroxyethyl)piperazine-1-ethanesulfonic acid, phytohemagglutinin M (PHA-M), sodium chloride, sodium citrate, HEPES, and phosphate-buffered saline (PBS) were purchased from Sigma-Aldrich (St. Louis, MO). Pluronic F127 (PF-127) and dimethyl sulfoxide (DMSO) were from D-BASF (Edinburgh, UK) and Fisher BioReagents (Fair Lawn, NJ), respectively. FTC (100% purity) was received as a gift from Gilead Sciences (Foster City, CA).

HeLa (ATCC CCL-2), H9 (ATCC HTB-176), and TZM-bl (PTA-5659) cell lines were purchased from the ATCC (Manassas, VA). RPMI 1640 medium, Dulbecco's high-glucose modified Eagle's medium (DMEM), fetal bovine serum (FBS), L-glutamine, trypsin, and penicillin-streptomycin (pen-strep) solution were purchased from HyClone (Logan, UT). Peripheral blood mononuclear cells (PBMCs) from healthy donors were isolated from whole blood by Histopaque-1077 (Sigma-Aldrich, St. Louis, MO) separation. PBMCs were further maintained in RPMI medium supplemented with 10% fetal bovine serum, 50 U/ml of interleukin 2 (IL-2), 8 mM L-glutamine, 100 U/ml of penicillin, and 100 μg/ml of streptomycin. For PBMCs, HIV-1_{LUC} was used to infect the cells (25). All reagents were used as received without further purification.

FTC-loaded PLGA NP formulation and characterization. FTC-loaded PLGA NPs (referred as FTC-NPs) were prepared by water-in-oil-in-water (W-O-W) emulsion method (36). Briefly, in the inner aqueous phase of W-O-W emulsion, 10 mg of FTC was dissolved in 2 ml of 1 mM HEPES buffer (pH 9). This showed enhanced FTC retention within the PLGA polymer. The inner aqueous phase was then added dropwise under constant magnetic stirring on 5 ml of organic phase (DCM) containing 100 mg of PLGA and PF-127 (stabilizer). After brief sonication, the water-in-oil (W-O) phase was added to the 20-ml outer aqueous phase of 1% PVA solution. The W-O-W emulsion was again sonicated for 5 min. The organic phase was eliminated by evaporation. Finally, the surfactants and free FTC were washed from NPs by dialysis (dialysis cassette with a molecular mass cutoff [CO] of 30 kDa; Thermo Scientific, Rockford, IL) within Milli-Q (MQ) water (18.2 MΩ). FTC-NPs were freeze-dried in the Millrock LD85 lyophilizer (Kingston, NY).

Physical-chemical characterization was performed to determine the size of NPs by dynamic light scattering (DLS), polydispersity index (PDI; a measure of the NP size heterogeneity in the given population), and zeta potential (i.e., surface charge of the NPs) of the NPs by using the ZetaPlus zeta potential analyzer (Brookhaven Instruments Corporation, Holtsville, NY). To carry out this analysis, an appropriate amount of freeze-dried FTC-NPs was dispersed in MQ water at room temperature. The data reported represent means ± standard errors (SE) obtained from 6 different batches.

The percent encapsulation efficiency (EE) and percent drug loading (DL) were evaluated by high-performance liquid chromatography (HPLC) analysis (Shimadzu, Kyoto, Japan). Briefly, FTC (absorbance of 280 nm, retention time of 3.38 min) loading concentrations in 1 mg of FTC-NPs dissolved in DMSO were estimated based on its respective standard curve determined by HPLC analysis (see "HPLC analysis" below) (37). The percent EE and percent DL were calculated by the following formulas:

$$\mathrm{EE} = \frac{(\text{amount of drug loaded in the NP})}{(\text{starting amount of drug})} \times 100 \quad (2)$$

$$\mathrm{DL} = \frac{(\text{amount of drug in the NPs})}{(\text{amount of polymer} + \text{drug})} \times 100 \quad (3)$$

The topography of the NPs was determined by scanning electronic microscopy (SEM) imaging (26). Briefly, the FTC-NP suspension was filtered through a Whatman Nuclepore track etch membrane with an ~50-nm pore size (Sigma-Aldrich, St. Louis, MO), and those NPs bearing membranes were air dried, mounted to an SEM stub, and sputter coated with a thin layer of chromium (thickness, ~3 to 5 nm). These NP-loaded membranes were imaged under a Hitachi S-4700 field emission SEM (Hitachi, New York, NY).

***In vitro* studies.** For various *in vitro* studies, H9 cells and PBMCs were cultured in RPMI medium, whereas HeLa and TZM-bl cells were maintained in DMEM. Both of the medium types were supplemented with 10% FBS, 1× L-glutamine, and 1× pen-strep solution unless otherwise indicated. For all experiments, cells were maintained in a humidified incubator with 5% CO_2 at 37°C. When necessary, cells were harvested by using 1× trypsin. All experiments were performed in triplicate, and FTC-NPs were compared with untreated control cells and FTC in solution.

Cytotoxicity assay. The cell cytotoxicity effect of FTC-NP was estimated by using the CellTiter-Glo luminescent cell viability assay method. Briefly, HeLa cells (10^5/ml), H9 cells (10^5/ml), and PBMCs (5×10^4/ml) were cultured overnight (O/N) in Nunc 96-well plates before treatment with FTC-NPs and FTC drug solution over different periods and at different concentrations. Further, as positive controls, wells were treated with 5% DMSO; negative-control wells contained untreated cells. The assay was performed by using the CellTiter-Glo luminescent cell viability assay kit (Promega, Madison, WI) according to the manufacturer's protocol. The luminescence was read after 30 min of reagent addition using a Synergy II multimode reader with Gen5 software (BioTek, Winooski, VT).

Endosomal pH-dependent FTC release studies. To evaluate endosomal FTC release efficacy of FTC-NP, 5 mg of FTC-NPs (with 47.5 μg of FTC entrapped) was dissolved in 1 ml of 20 mM citrate buffer (pH 5.5). After the desired period (1 h or 1, 7, 14, or 30 days), 200 μl of supernatant was collected and the amount of FTC release was evaluated by HPLC by following the methodology explained in "HPLC analysis" below. This study was carried out on 3 different batches of FTC-NPs. The percent FTC at each time point was analyzed by the following equations:

$$\text{FTC release at 1 h} = \frac{(\text{amount of FTC in 200 μl of supernatant})}{(\text{amount of FTC in 5 mg of FTC-NPs in 1 ml})} \times 100 \quad (4)$$

$$\text{FTC release at day 7, 14, or 30} = \frac{(\text{amount of FTC in 200 μl of supernatant})}{(\text{amount of FTC in FTC-NPs retained in respective volume})} \times 100 \quad (5)$$

To maintain the sink condition, the volume was not readjusted. Therefore, on days 7, 14, and 30, the amount of FTC released from FTC-NPs was determined in respective volumes corresponding to 800, 600, and 400 μl. A removal of a 200-μl volume leads to removal of FTC in that volume. Therefore, at each time point the FTC amount in the respective volume was subtracted from the sink.

Intracellular FTC retention studies. For *in vitro* concentration-dependent and time-dependent uptake and drug retention studies, TZM-bl cells (10^5/ml) were seeded in Nunc 6-well plates and kept O/N for adherence before treatment. For concentration-dependent studies, TZM-bl cells were treated at 0.001, 0.01, 0.1, 1, and 10 μg/ml of FTC, as FTC-NPs and FTC solution, for 24 h. For time-dependent studies, HeLa cells were treated with FTC-NPs (at 10 μg/ml of FTC) for 20 min, 24 h, 48 h, and 96 h. After the treatment period, triplicate wells were washed thrice with 1× PBS, followed by ACN-mediated cell lysis and protein precipitation. Cell extracts were subjected to a solid-phase extraction (SPE) purification

method by using protein precipitation plates (Thermo Scientific, Rockford, IL), and the drug concentration was analyzed using HPLC (see below).

HPLC analysis. HPLC was used both to determine FTC loading efficiency in FTC-NPs and to determine intracellular FTC retention. Briefly, the chromatographic separation was performed with a Phenomenex (Torrance, CA) C_{18} (150 by 4.6 mm; particle size, 5 μm) column under isocratic elution conditions by using a mixture of ACN and 25 mM KH_2PO_4 solution (55:45, vol/vol). The column was maintained at flow rate of 0.5 ml/min and a temperature of 25°C; and FTC detection was performed by using a UV detector at 280 nm. Quantification was based on analysis of the area under the curve (AUC). The amount released was analyzed based on the standard curve construction by running pure FTC solution at the concentration range of 0.0004 to 0.25 mg/ml (a linear correlation having an r^2 of 0.99, with a retention time of 3.38 min). The HPLC instrument was equipped with LC-20AB pumps, an SIL-20AC autosampler, and an SPD-20A UV-visible detector. The instrument interday and intraday variability was <10%. For percent EE and percent DL of FTC in FTC-NPs, data were obtained from 4 independent experiments, whereas for intercellular FTC retention, data were obtained from 3 independent experiments.

***In vitro* prophylaxis study.** Short-term (1 day pretreatment) *in vitro* prophylaxis of FTC-NPs versus FTC solution against HIV-1_{NL4-3} was performed using TZM-bl cells as HIV-1 infection indicator cells (37). Briefly, TZM-bl cells (10^5/ml) were seeded in a 96-well plate. After O/N incubation, cells were treated with different FTC concentrations (0.001 to 10 μg/ml) as FTC-NPs and FTC solution. After 24 h of treatment, the cells were washed thrice with warm PBS, followed by inoculation with HIV-1_{NL4-3} (100 ng) for 4 h. The cells were again washed as described above and incubated in fresh medium. However, PBMCs (2×10^6 cells/ml) isolated from three different donors were first stimulated with PHA (2 μg/ml) and IL-2 (50 U/ml) for 48 h and then treated with different FTC concentrations (0.001 to 10 μg/ml) as FTC-NPs and FTC solution for 24 h. PBMCs were then infected with HIV-1_{LUC} (100 ng) for 4 h, washed thrice with warm PBS, and resuspended in fresh medium and allowed to incubate for 96 h. A process similar to that for TZM-bl cells was followed. For both studies, untreated uninfected cells and untreated infected cells were used as negative and positive controls, respectively. After 96 h of incubation as a measure of HIV-1 infection, duplicate wells were used for determination of the luminescence using the BrightGLO (Promega, Madison, WI) assay. A Synergy HT multimode microplate reader (BioTek, Winooski, VT) was used to read the luminescence. Luminescence was determined as relative luminescence units (RLU). The percent protection from HIV-1 infection was calculated by using the equation below:

$$\text{HIV-1 inhibition (percent protection from HIV-1 infection)} = \frac{(L_{\text{untreated}} - L_{\text{treated}})}{L_{\text{untreated}}} \times 100 \qquad (6)$$

where $L_{\text{untreated}}$ is the luminescence of untreated but HIV-1-infected TZM-bl cells or PBMCs (untreated infected cells) and L_{treated} is the luminescence of respective FTC-NP- and FTC solution-treated plus HIV-1-infected TZM-bl cells or HIV-1_{LUC}-infected PBMCs (treated infected cells). The results of these experiments are shown as means ± SE from three independent experiments.

exo-RT activity quantification by [^{32}P]TTP incorporation assay. To test FTC-NP efficacy, 2×10^7 PBMCs were seeded per well in a 24-well plate and were treated for 18 h with 500 ng/ml of FTC solution, 500 ng/ml of FTC entrapped in FTC-NPs, and an equivalent volume of 1× PBS (control). The PBMCs were washed with warm PBS and resuspended in fresh complete RPMI medium, followed by inoculation with 100 ng of HIV-1_{NL4-3} (38) for 6 h. The treated infected PBMCs were washed with warm PBS and were maintained in complete RPMI medium. At the desired time point (0, 3, 7, 10, 14, 17, and 21 days), virus replication was monitored by sampling supernatants in triplicate and measuring exogenous RT (exo-RT) activity using an [^{32}P]TTP (PerkinElmer, MA) incorporation assay as described previously (39), except that reaction mixtures were spotted onto DE81 filter paper (Thermo Fisher, Waltham, MA) and washed thrice with 2× SSC (pH 7; 01× SSC is 0.15 M NaCl plus 0.015 M sodium citrate) and once with 95% ethanol. Activity was quantified by phosphorimage analysis using a Typhoon 9410 imager and ImageQuant software (GE Healthcare, Pittsburgh, PA).

$$\text{exo-RT activity} = [^{32}\text{P}]\text{TTP at respective time point} - [^{32}\text{P}]\ \text{TTP at respective time zero} \qquad (7)$$

Statistical analysis. All experiments were performed at least in triplicate. Respective graph represents values as means ± SE of the obtained data. For cellular experiments, data were analyzed by one-way analysis of variance (ANOVA) followed by *post hoc* (Bonferroni's multiple-comparison test) and Pearson's correlation by using GraphPad Prism 5 software (GraphPad, La Jolla, CA). However, for infection studies, 50% inhibitory concentration (IC_{50}) was analyzed based on log(agonist) versus response. The significant differences among treated and control groups at different concentrations and over time were considered to be statistically significant at a P value of <0.05. The half-life calculation for endosomal FTC release was analyzed based on one phase decay fitting.

ACKNOWLEDGMENTS

This project and publication were funded by NIAID R01AI117740-01, 2015 (to C.J.D.).

The following reagent was obtained through the AIDS Reagent Program, Division of AIDS, NIAID, NIH: HIV-1_{LAI} from Jean-Marie Bechet and Luc Montagnier.

We report no conflicts of interest in this work.

REFERENCES

1. Cahn P. 2004. Emtricitabine: a new nucleoside analogue for once-daily antiretroviral therapy. Expert Opin Invest Drugs 13:55–68. https://doi.org/10.1517/13543784.13.1.55.
2. Buckhold FR, III. 2015. Primary care of the human immunodeficiency virus patient. Med Clin North Am 99:1105–1122. https://doi.org/10.1016/j.mcna.2015.05.010.
3. UNAIDS. 2015. Fact sheet 2015. UNAIDS, Geneva, Switzerland. http://www.unaids.org/sites/default/files/media_asset/20150901_FactSheet_2015_en.pdf.
4. AIDSinfo. 2014. Guidelines for the use of antiretroviral agents in HIV-1-infected adults and adolescents. AIDSinfo, Rockville, MD. https://aidsinfo.nih.gov/guidelines/html/1/adult-and-adolescent-arv-guidelines/30/adherence-to-art. Accessed 4 October 2016.
5. Wang LH, Begley J, St Claire RL, III, Harris J, Wakeford C, Rousseau FS. 2004. Pharmacokinetic and pharmacodynamic characteristics of emtricitabine support its once daily dosing for the treatment of HIV infection. AIDS Res Hum Retroviruses 20:1173–1182. https://doi.org/10.1089/aid.2004.20.1173.
6. Jordan J, Carranza-Rosenzweig J, Pathak D, Pilon T. 2000. Perceived influence of regimen characteristics on adherence, abstr P121. Program Abstr 5th Int Congr Drug Ther HIV Infect, Glasgow, United Kingdom.
7. Duan J, Freeling JP, Koehn J, Shu C, Ho RJ. 2014. Evaluation of atazanavir and darunavir interactions with lipids for developing pH-responsive anti-HIV drug combination nanoparticles. J Pharm Sci 103:2520–2529. https://doi.org/10.1002/jps.24046.
8. Dash PK, Gendelman HE, Roy U, Balkundi S, Alnouti Y, Mosley RL, Gelbard HA, McMillan J, Gorantla S, Poluektova LY. 2012. Long-acting nanoformulated antiretroviral therapy elicits potent antiretroviral and neuroprotective responses in HIV-1-infected humanized mice. AIDS 26:2135–2144. https://doi.org/10.1097/QAD.0b013e328357f5ad.
9. Mandal, S, Zhou, Y, Shibata, A, Destache, CJ. 2015. Confocal fluorescence microscopy: an ultra-sensitive tool used to evaluate intracellular antiretroviral nano-drug delivery in HeLa cells. AIP Adv 5:084803. https://doi.org/10.1063/1.4926584.
10. Freeling JP, Koehn J, Shu C, Sun J, Ho RJY. 2014. Long-acting three-drug combination anti-HIV nanoparticles enhance drug exposure in primate plasma and cells within lymph nodes and blood. AIDS 28:2625–2627. https://doi.org/10.1097/QAD.0000000000000421.
11. Makadia HK, Siegel SJ. 2011. Poly lactic-co-glycolic acid (PLGA) as biodegradable controlled drug delivery carrier. Polymers (Basel) 3:1377–1397. https://doi.org/10.3390/polym3031377.
12. Destache CJ, Belgum T, Goede M, Shibata A, Belshan MA. 2010. Antiretroviral release from poly(DL-lactide-co-glycolide) nanoparticles in mice. J Antimicrob Chemother 65:2183–2187. https://doi.org/10.1093/jac/dkq318.
13. Danhier F, Lecouturier N, Vroman B, Jerome C, Marchand-Brynaert J, Feron O, Preat V. 2009. Paclitaxel-loaded PEGylated PLGA-based nanoparticles: in vitro and in vivo evaluation. J Control Release 133:11–17. https://doi.org/10.1016/j.jconrel.2008.09.086.
14. Schinazi RF, Bassit L, Clayton MM, Sun B, Kohler JJ, Obikhod A, Arzumanyan A, Feitelson MA. 2012. Evaluation of single and combination therapies with tenofovir disoproxil fumarate and emtricitabine in vitro and in a robust mouse model supporting high levels of hepatitis B virus replication. Antimicrob Agents Chemother 56:6186–6191. https://doi.org/10.1128/AAC.01483-12.
15. Agarwal R, Singh V, Jurney P, Shi L, Sreenivasan SV, Roy K. 2013. Mammalian cells preferentially internalize hydrogel nanodiscs over nanorods and use shape-specific uptake mechanisms. Proc Natl Acad Sci U S A 110:17247–17252. https://doi.org/10.1073/pnas.1305000110.
16. Chen TR. 1992. Karyotypic derivation of H9 cell line expressing human immunodeficiency virus susceptibility. J Natl Cancer Inst 84:1922–1926. https://doi.org/10.1093/jnci/84.24.1922.
17. Hart GJ, Orr DC, Penn CR, Figueiredo HT, Gray NM, Boehme RE, Cameron JM. 1992. Effects of (−)-2′-deoxy-3′-thiacytidine (3TC) 5′-triphosphate on human immunodeficiency virus reverse transcriptase and mammalian DNA polymerases alpha, beta, and gamma. Antimicrob Agents Chemother 36:1688–1694. https://doi.org/10.1128/AAC.36.8.1688.
18. Margolis AM, Heverling H, Pham PA, Stolbach A. 2014. A review of the toxicity of HIV medications. J Med Toxicol 10:26–39. https://doi.org/10.1007/s13181-013-0325-8.
19. US FDA. 2003. Center for Drug Evaluation and Research approval package for application number: 21-500. Microbiology review. Division of Antiviral Drug Products (HFD-530), Center for Drug Evaluation and Research, Silver Spring, MD. http://www.accessdata.fda.gov/drugsatfda_docs/nda/2003/21-500_Emtriva_Microbr.pdf.
20. Georgiev VS. 2009. NIAID: international involvement in HIV/AIDS research, p. 387. *In* National Institute of Allergy and Infections Diseases, NIH: impact on global health, vol 2. Humana Press, New York, NY.
21. Cohen C, Wohl D, Arribas JR, Henry K, Van Lunzen J, Bloch M, Towner W, Wilkins E, Ebrahimi R, Porter D, White K, Walker I, Chuck S, De-Oertel S, Fralich T. 2014. Week 48 results from a randomized clinical trial of rilpivirine/emtricitabine/tenofovir disoproxil fumarate vs. efavirenz/emtricitabine/tenofovir disoproxil fumarate in treatment-naive HIV-1-infected adults. AIDS 28:989–997. https://doi.org/10.1097/QAD.0000000000000169.
22. Saag MS, Cahn P, Raffi F, Wolff M, Pearce D, Molina JM, Powderly W, Shaw AL, Mondou E, Hinkle J, Borroto-Esoda K, Quinn JB, Barry DW, Rousseau F. 2004. Efficacy and safety of emtricitabine vs stavudine in combination therapy in antiretroviral-naive patients: a randomized trial. JAMA 292:180–189. https://doi.org/10.1001/jama.292.2.180.
23. Kulkarni R, Hluhanich R, McColl DM, Miller MD, White KL. 2014. The combined anti-HIV-1 activities of emtricitabine and tenofovir plus the integrase inhibitor elvitegravir or raltegravir show high levels of synergy in vitro. Antimicrob Agents Chemother 58:6145–6150. https://doi.org/10.1128/AAC.03591-14.
24. Gilead Sciences. 2013. TRUVADA prescribing information. http://www.gilead.com/~/media/files/pdfs/medicines/hiv/truvada/truvada_pi.pdf?la=en. Accessed 17 October 2016.
25. Barré-Sinoussi F, Chermann JC, Rey F, Negeyre MT, Chamaret S, Gruest J, Dauguet C, Axler-Blin C, Cezinet-Brus F, Rouzioux C, Rozenbaum W, Montagnier L. 1983. Isolation of a T-lymphotropic retrovirus from a patient at risk for acquired immune deficiency syndrome (AIDS). Science 220:868–871.
26. Shibata A, McMullen E, Pham A, Belshan M, Sanford B, Zhou Y, Goede M, Date AA, Destache CJ. 2013. Polymeric nanoparticles containing combination antiretroviral drugs for HIV type 1 treatment. AIDS Res Hum Retroviruses 29:746–754. https://doi.org/10.1089/aid.2012.0301.
27. Freeling JP, Koehn J, Shu C, Sun J, Ho RJ. 2015. Anti-HIV drug-combination nanoparticles enhance plasma drug exposure duration as well as triple drug combination levels in cells within lymph nodes and blood in primates. AIDS Res Hum Retroviruses 31:107–114. https://doi.org/10.1089/aid.2014.0210.
28. Puligujja P, Arainga M, Dash P, Palandri D, Mosley RL, Gorantla S, Poluektova L, McMillan J, Gendelman HE. 2015. Pharmacodynamics of folic acid receptor targeted antiretroviral nanotherapy in HIV-1-infected humanized mice. Antiviral Res 120:85–88. https://doi.org/10.1016/j.antiviral.2015.05.009.
29. Puligujja P, Balkundi SS, Kendrick LM, Baldridge HM, Hilaire JR, Bade AN, Dash PK, Zhang G, Poluektova LY, Gorantla S, Lui XM, Ying T, Feng Y, Want Y, Dimitrov DS, McMillan JM, Gendelman HE. 2015. Pharmacodynamics of long-acting folic acid-receptor targeted ritonavir-boosted atazanavir nanoformulations. Biomaterials 41:141–150. https://doi.org/10.1016/j.biomaterials.2014.11.012.
30. Eslava-Kim L. 2015. Promising results for first long-acting all-injectable HIV combo drug. http://www.empr.com/drugs-in-the-pipeline/promising-results-for-first-long-acting-all-injectable-hiv-combo-drug/article/451488/.
31. Ford N, Shubber Z, Hill A, Vitoria M, Doherty M, Mills EJ, Gray A. 2013. Comparative efficacy of lamivudine and emtricitabine: a systematic review and meta-analysis of randomized trials. PLoS One 8:e79981. https://doi.org/10.1371/journal.pone.0079981.
32. Ford N, Flexner C, Vella S, Ripin D, Vitoria M. 2013. Optimization and simplification of antiretroviral therapy for adults and children. Curr Opin HIV AIDS 8:591–599. https://doi.org/10.1097/COH.0000000000000010.
33. Plosker GL. 2013. Emtricitabine/tenofovir disoproxil fumarate: a review of its use in HIV-1 pre-exposure prophylaxis. Drugs 73:279–291. https://doi.org/10.1007/s40265-013-0024-4.
34. Bose T, Latawiec D, Mondal PP, Mandal S. 2014. Overview of nano-drugs characteristics for clinical application: the journey from the entry to the exit point. J Nanoparticle Res 16:2527. https://doi.org/10.1007/s11051-014-2527-7.
35. Kim RB. 2003. Drug transporters in HIV therapy. Top HIV Med 11:136–139.
36. Govender T, Stolnik S, Garnett MC, Illum L, Davis SS. 1999. PLGA nano-

particles prepared by nanoprecipitation: drug loading and release studies of a water soluble drug. J Control Release 57:171–185. https://doi.org/10.1016/S0168-3659(98)00116-3.
37. Singh G, Pai RS. 2014. Optimization (central composite design) and validation of HPLC method for investigation of emtricitabine loaded poly(lactic-co-glycolic acid) nanoparticles: in vitro drug release and in vivo pharmacokinetic studies. ScientificWorldJournal 2014:583090.
38. Brown HE, Chen H, Engelman A. 1999. Structure-based mutagenesis of the human immunodeficiency virus type 1 DNA attachment site: effects on integration and cDNA synthesis. J Virol 73:9011–9020.
39. Belshan M, Schweitzer CJ, Donnellan MR, Lu R, Engelman A. 2009. In vivo biotinylation and capture of HIV-1 matrix and integrase proteins. J Virol Methods 159:178–184. https://doi.org/10.1016/j.jviromet.2009.03.017.